Active loop extrusion modulates the mechanical response of chromatin under tension

Hossein Salari [*]
Laboratoire de Biologie et Modélisation de la Cellule, École Normale Supérieure de Lyon, CNRS, UMR5239, Inserm U1293, Université Claude Bernard Lyon 1, 46 Allée d'Italie, 69007 Lyon, France and Institut Curie, PSL Research University, CNRS UMR3244, Dynamics of Genetic Information, Sorbonne Université, 75005 Paris, France

Daniel Jost [†]
Laboratoire de Biologie et Modélisation de la Cellule, École Normale Supérieure de Lyon, CNRS, UMR5239, Inserm U1293, Université Claude Bernard Lyon 1, 46 Allée d'Italie, 69007 Lyon, France

(Received 16 September 2025; accepted 14 November 2025; published 20 February 2026)

Chromosomes are complex biopolymers folded into dynamic loops via a loop-extrusion process and may experience various mechanical forces *in vivo*. We develop a force-dependent model of chromatin loop extrusion and investigate its mechanical consequences on chromosome organization using simulations and analytical theory. We show that loop extrusion alters the force-extension behavior of DNA in a nonmonotonic manner: Extrusion stiffens the chain at low forces but softens it at intermediate and high forces. Our model predicts hysteresis in pulling-recoiling cycles and out-of-equilibrium responses, qualitatively consistent with recent single-chromosome stretching experiments. We further find that loop extrusion provides mechanical robustness to chromatin by promoting compaction while enabling rapid structural recovery after stress. These results establish loop extrusion as a key regulator of chromatin mechanics.

DOI: 10.1103/qfdv-vhv1

I. INTRODUCTION

The three-dimensional (3D) organization of the genome plays a fundamental role in regulating essential cellular processes, including gene transcription [1], DNA replication [2], and repair [3,4]. However, chromatin—the nucleoprotein polymer forming chromosomes—is not a static scaffold: It is dynamically remodeled and is frequently subjected to mechanical forces generated by various processes such as pulling centromeres by microtubule spindles during mitosis [5], cytoskeleton-mediated nuclear deformations that affect chromatin in the nuclear periphery [6], or the actions of different molecular motors on chromatin substrate such as DNA and RNA polymerases [7,8]. These forces can impose significant tensile stresses on the genome [9]. How chromatin preserves its structural and functional integrity under such mechanical challenges remains a central question in genome biology.

A key mechanism driving 3D genome organization is DNA loop extrusion, an ATP-dependent process mediated by structural maintenance of chromosomes (SMC) complexes such as cohesin and condensin [10] that organizes chromatin into topologically associating domains and regulatory loops [11,12]. Although the precise molecular basis of SMC-driven loop extrusion remains under debate, several mechanistic models have been proposed, notably the scrunching model. In this model, the SMC complex remains stationary on DNA while conformational changes "reel in" the DNA to enlarge the loop. DNA binds at two sites (e.g., hinge and head domains), and ATP binding drives the hinge toward the heads, pulling DNA inward [10].

Many *in vitro* experiments on naked DNA have shown that increasing mechanical tension on the DNA template substantially slows down loop-extrusion activity [13,14]. For instance, Ganji *et al.* observed that the condensin extrusion rate decreases from ∼1.5 kb/s at ∼0.1 pN to ∼0.1 kb/s at ∼0.7 pN, suggesting a subpiconewton stall force for condensin-mediated loop extrusion.

In recent years, the interplay between enzymatic activity and polymer rheology has attracted growing attention [15,16]. Loop extrusion, in particular, may enable chromatin to dynamically adjust its organization in response to mechanical stress. Recent studies have shown that condensin I enhances the stiffness and stability of mitotic chromosomes [17], pointing to a potential role for loop extrusion in resisting force-induced decompaction. Yet, the mechanistic coupling between chromatin mechanics and loop-extrusion activity remains largely unexplored.

In this work, we present a polymer model of chromatin that incorporates force-dependent loop-extrusion activity. Inspired by recent experiments *in vivo* and *in vitro* that examined the mechanical response of chromosomes under applied tension [18,19], we systematically characterize the force-extension (FE) relation of loop-extruded chromatin using simulations

[*]Contact author: hossein.salari@curie.fr
[†]Contact author: daniel.jost@ens-lyon.fr

Published by the American Physical Society under the terms of the Creative Commons Attribution 4.0 International license. Further distribution of this work must maintain attribution to the author(s) and the published article's title, journal citation, and DOI.

and polymer theory. This framework allows us to investigate how loop extrusion modulates the stiffness of the chromatin and contributes to its mechanical resilience.

II. MODEL

We developed a 3D polymer model of chromatin under tension (see the "Method" section in the Supplemental Material [20]). Following our previous work [21,22], chromatin is modeled as a semiflexible (Kuhn length $l_k = 100$ nm), self-avoiding chain. Each monomer, 20 nm in size, corresponds to 1 kb of genomic DNA [Fig. 1(a)] and evolves over time via standard kinetic Monte Carlo (MC) simulations, with one MC step equal to ∼1 ms in real time (see Fig. S1 of the Supplemental Material [20]).

To model loop extrusion, we adopt a standard coarse-grained translocation scheme [21,23]. Loop-extruding factors (LEFs) bind and unbind to chromatin at rates k_b and k_u, respectively [Fig. 1(a)]. At steady state, the probability of LEF binding is given by $\rho = k_b/(k_b + k_u)$, and the mean number of bound LEFs is $\bar{n} = N_e\rho$, where N_e is the total number of LEFs. Upon binding, one LEF anchors its two "legs" to adjacent monomers and extrudes a loop by stochastically translocating the leg positions along the chain away from each other at a characteristic velocity v_e. This movement can be one-sided or two-sided, depending on the extrusion mechanism. At steady state, the average residence time of an LEF on DNA is $1/k_u$, and its processivity, defined as the average extruded loop size in the absence of any barrier, is given by $p = v_e/k_u$.

To maintain physical connectivity between the LEF legs, we introduce a harmonic spring between them, of stiffness K_{smc} that models effectively the topological entrapment of the polymer chain within the SMC ring of the LEF. Legs of different LEFs may pass through one another depending on a crossing probability α, ranging from 0 (no possible crossing) to 1 (phantom legs). Translocation of a leg halts when it encounters a boundary element. Note that, in this coarse-grained translocation model, LEFs connect two polymer monomers without requiring the chromatin strand to pass through the SMC ring.

To simulate mechanical stretching, equal and opposite external forces of strength F_{ext} are applied at the two opposite ends of the chain.

Within this framework, the local force exerted on an LEF at a given time, F_{smc}, is $F_{\mathrm{smc}} = K_{\mathrm{smc}}\,(x_{\mathrm{smc}} - x_0)$, where x_{smc} is the current spatial separation between the two legs, and $x_0 = 20$ nm is the rest length of the spring. We choose $K_{\mathrm{smc}} = 0.031$ pN/nm consistent with recent *in vitro* experiments estimating that a displacement of ∼32 nm between cohesin's head and hinge domains (the two possible legs) generates a restoring force of ∼1 pN [24,25].

To incorporate force-dependent extrusion activity into the model, we assume that the extrusion velocity decreases exponentially with the force experienced by the LEF:

$$v_e = v_e^0 \exp\left(-\frac{F_{\mathrm{smc}}}{F_e}\right),$$

where v_e^0 is the extrusion velocity in the absence of force and F_e is the characteristic force-scale determining the sensitivity of LEFs to mechanical load. By fitting this model to available experimental data on the force dependency of the velocity of condensin [14] (see Fig. S2 of the Supplemental Material [20]), we found $v_e^0 \approx 1.1$ kb/s and $F_e \approx 0.2$ pN. Notably, the value of F_e aligns well with the reported stall force of condensin [14].

We also extend this reasoning to LEF unbinding kinetics. As DNA tension may destabilize protein-DNA interactions, we assume that the unbinding rate increases exponentially with force:

$$k_u = k_u^0 \exp\left(\frac{F_{\mathrm{smc}}}{F_u}\right),$$

where k_u^0 is the unbinding rate in the absence of tension and F_u denotes the characteristic force scale governing the sensitivity of unbinding to tension. In the absence of direct experimental measurements of F_u, we assume that LEF dissociation is less sensitive to force than loop extrusion ($F_u > F_e$). Accordingly, we explore a range of F_u values: 0.65, 1.31, and 13.1 pN.

With this model, we investigate the behavior of a 500-kb-long chromatin segment with fixed boundary elements at each end, at steady state. The applied external force is systematically varied quasistatically from 0 to 1 pN. Two loop-extrusion regimes are considered: a "low"-activity regime with zero-force processivity $p_0 = v_e^0/k_u^0 = 250$ kb and mean LEF number $\bar{n}_0 = 2.5$, and a "high"-activity regime with $p_0 = 500$ kb and $\bar{n}_0 = 5.0$. For both regimes, we simulate both one-sided (only one leg, randomly chosen, can translocate at velocity v_e) and two-sided (both legs can translocate, each at velocity $v_e/2$) loop-extrusion scenarios for $\alpha = 0$ and $\alpha = 1$. Additionally, we vary the zero-force extrusion velocity v_e^0 across a wide range—[1.0, 10, 100] kb/s—to systematically explore how loop-extrusion speed may influence chromatin mechanics.

III. RESULTS

A. Loop extrusion alters chromatin mechanics by tuning stored length

Overall, simulations reveal that the decrease of LEF speed and dwell time under tension leads to a reduction in the average loop sizes and numbers as well as in the fraction of DNA engaged inside loops [Fig. 1(b) and Fig. S3 of the Supplemental Material [20]].

To assess the mechanical impact of loop extrusion, we derive the FE curves of the polymer for each investigated set of parameters [Fig. 1(c) and Fig. S4 of the Supplemental Material [20], colored symbols]. In all cases, the FE curve differs qualitatively from the situation without LEFs (black symbols), exhibiting a characteristic "tildelike" shape. In particular, for a given applied force, the extruded polymer exhibits a lower extension because of the compaction mediated by loop formation. This compaction is more pronounced in the "high"-activity regime and is slightly stronger for two-sided extrusion than for one-sided. Moreover, the effect is amplified when LEF legs are allowed to cross one another ($\alpha = 1$ vs $\alpha = 0$). Finally, we find that increasing the unbinding force scale F_u enhances this behavior (Fig. S5 of the Supplemental Material [20]). Across all tested parameters—including extrusion directionality, crossing probability, and F_u—the overall "tildelike" shape of the FE curve is preserved, with these

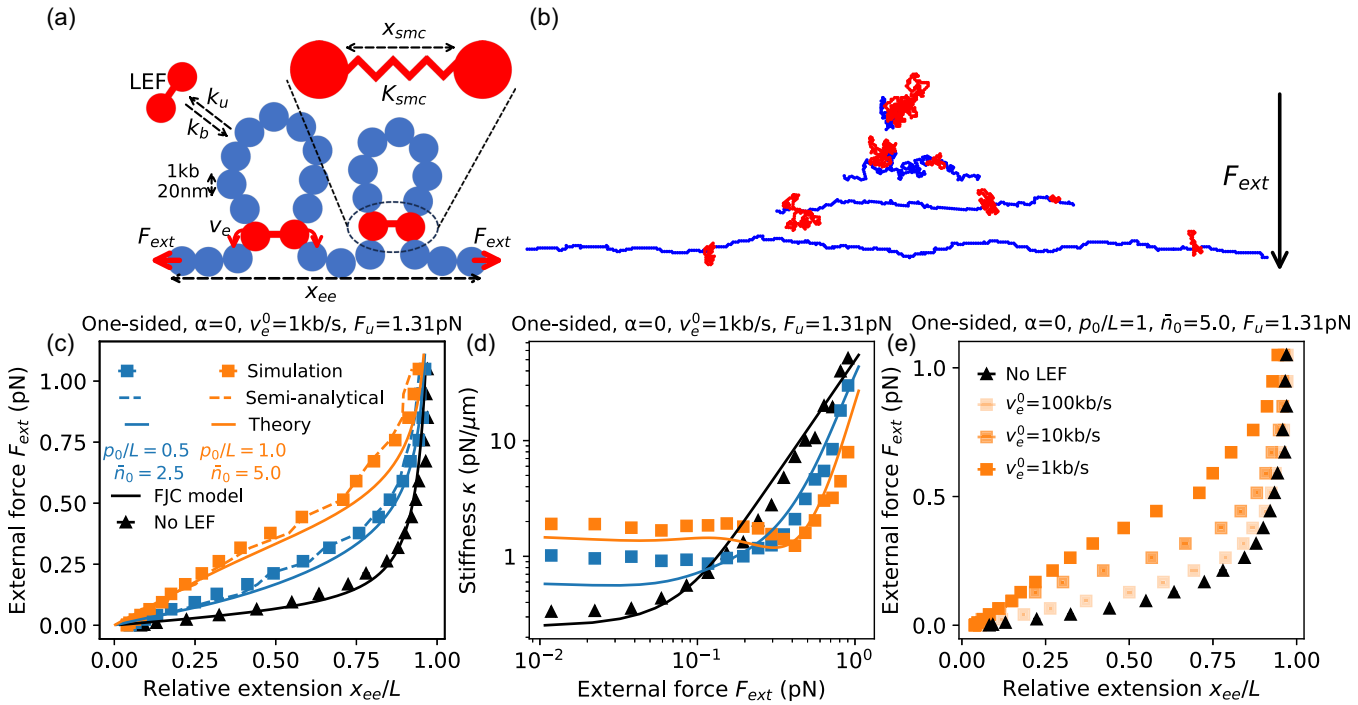


FIG. 1. Anomalous force-extension curve induced by loop-extrusion activity. (a) Schematic representation of the polymer model under tension with SMC-mediated loop extrusion. (b) Representative snapshots of the polymer under increasing external forces. Extruded segments are shown in red; nonextruded segments in shown in blue. (c) Force-extension curves for different loop-extrusion activities. Symbols represent simulation results; curves denote theoretical predictions. (d) Effective stiffness κ as a function of external force, extracted from the force-extension data shown in panel (c). Same color legend as in panel (c). (e) Comparison of force-extension curves for various zero-force extrusion speeds v_e^0 in the high-activity regime and in the one-sided and $\alpha = 0$ case. Symbols represent simulation results.

parameters primarily modulating the strength of the observed features rather than altering their qualitative form.

We show that the FE behavior of a chain without loop extrusion is accurately captured by the freely jointed chain (FJC) model with $l_k = 100\,\mathrm{nm}$ [Fig. 1(c)]. Building on this agreement, we extend the FJC framework to incorporate the effects of loop extrusion. The extension (projection of end-to-end distance along the force direction) x_{ee} of an FJC under tension is given by [26]

$$x_{\mathrm{ee}} = L_c\left(\coth\left(\frac{F_{\mathrm{ext}} l_k}{k_{\mathrm{B}}T}\right) - \frac{k_{\mathrm{B}}T}{F_{\mathrm{ext}} l_k}\right), \tag{1}$$

where L_c is the contour length of the polymer, k_{B} is the Boltzmann constant, and T is the absolute temperature.

In the presence of active loop extrusion, a fraction of the DNA is dynamically sequestered within loops, reducing the effective contour length L_c^{eff} available for extension. From simulations, we can estimate directly L_c^{eff} and then predict the extension via the FJC model [dashed curves in Fig. 1(c)]. This semianalytical approach demonstrates that the primary effect of loop extrusion on the FE curve can be interpreted as a reduction in the effective contour length.

To obtain a theoretical prediction for L_c^{eff}, we consider a chromatin domain of length L with $\bar{n}$ LEFs, either two-sided or one-sided. For two-sided LEFs, we assume that the domain is partitioned into $\bar{n}$ equal subdomains of size $L/\bar{n}$, with each LEF acting independently within its subdomain. For one-sided LEFs, the effective number of extruding legs is halved, so the domain is divided into $\bar{n}/2$ subdomains of size $2L/\bar{n}$. In this framework, the average loop size extruded by a single LEF can be approximated as (see the Supplemental Material [20])

$$\begin{aligned}\langle l\rangle_{\mathrm{two}} &\approx p(1-\exp(-L/\bar{n}p)),\\ \langle l\rangle_{\mathrm{one}} &\approx p(1-\bar{n}p/2L(1-\exp(-2L/\bar{n}p))),\end{aligned} \tag{2}$$

where $\langle\cdot\rangle$ denotes the ensemble average. The total fraction of DNA engaged within extruded loops can then be estimated by multiplying the number of LEFs by the average loop size.

Since both p and $\bar{n}$ are force dependent, we assume the applied external force F_{ext} is uniformly transmitted along the chain, and each LEF experiences this force. Accordingly, we express the force-dependent processivity and LEF occupancy as

$$\begin{aligned}p(F_{\mathrm{ext}}) &= p_0\exp(-F_{\mathrm{ext}}(F_u+F_e)/F_uF_e),\\ \bar{n}(F_{\mathrm{ext}}) &= N_e k_b/(k_b + k_u^0\exp(F_{\mathrm{ext}}/F_u)).\end{aligned} \tag{3}$$

Notably, despite this simplifying assumption, the analytical predictions qualitatively match the Monte Carlo simulation results in both "low" and "high" loop-extrusion activity regimes [Fig. 1(c) and Fig. S3 of the Supplemental Material [20]], indicating that the uniform-force approximation captures the average behavior of the system effectively.

B. Nonmonotonic force-dependent chromatin stiffness

We further evaluate the stiffness of the polymer under loop extrusion, defined as $\kappa = \partial F_{\mathrm{ext}}/\partial x_{\mathrm{ee}}$ [Fig. 1(d)]. For an ideal

FJC without loop extrusion, stiffness exhibits two regimes: At low forces, κ is approximately constant, while at high forces, $\kappa \sim F_{\text{ext}}^2$. When loop extrusion is active, we observe an enhancement of stiffness in the low-force regime, which becomes more pronounced with increasing extrusion activity. This behavior reflects the tendency of LEFs to resist chain extension by compacting the polymer into loops. In contrast, for larger applied forces, above F_e, the stiffness becomes lower than that of the ideal chain. Interestingly, the force-stiffness relationship becomes nonmonotonic: κ reaches a local minimum at an intermediate force regime before rising again at high forces. This behavior is especially pronounced for systems with "high" loop-extrusion activity. Indeed, when loops start to be disrupted near the stall force, the sudden release of the monomers stored within the loops leads to a sharp increase in the effective contour length and thus a transient softening of the polymer [27]. Finally, at very high forces, all stiffness curves converge to the ideal chain behavior, indicating that LEFs become effectively inactive under strong tension.

C. Impact of loop-extrusion speed on chromatin mechanics

Next, we investigate how the zero-force loop-extrusion speed v_e^0 influences the effective stiffness of the polymer [Fig. 1(e)], adjusting k_u^0 to maintain fixed p_0 and $\bar{n}_0$ values. We find that the impact of loop extrusion on the FE diminishes as v_e^0 augments and both the actual average number and size of extruded loops decrease with v_e^0 [Fig. S6 of the Supplemental Material [20]]. This translates in part to an important reduction in LEF stability on the polymer caused by strong stresses acting on the LEF spring. Indeed, at high speed, the characteristic timescale of loop extrusion activity, $t_e \sim 1\,\text{kbp}/v_e$, becomes shorter than the polymer relaxation time, which is approximately $t_p \approx 0.5$ s in our simulations (estimated from the relaxation dynamics of the end-to-end distance of a 100-kbp DNA; Fig. S7 of the Supplemental Material [20]). As a result, the legs of the LEF may not have sufficient time to reach their equilibrium configuration, leading to transiently strong deformation of the spring and thus elevated internal forces F_{smc}. These nonequilibrium forces increase the unbinding rate in addition to reducing the effective extrusion rate, thereby lowering the functional processivity. Consequently, LEFs with high v_e^0 may not form significantly large chromatin loops before detaching, thereby limiting their contribution to the overall mechanical response of the polymer.

D. Loop extrusion enhances chromatin stability under tension

To explore how loop extrusion stabilizes chromatin under mechanical tension, we compute the contact probability within a chromatin domain subjected to varying external forces [Fig. 2(a) and Fig. S8(a) of the Supplemental Material [20]]. In the absence of loop extrusion, even weak forces (as low as ∼0.1 pN) lead to a dramatic loss of contacts, indicating significant conformational changes. In contrast, when loop extrusion is active, the polymer structure remains largely unaffected up to forces of approximately 0.3 pN.

To further assess structural stability, we introduce a pair of "sticky" monomers—representing regulatory elements such as an enhancer and a promoter—separated by 100 kb and

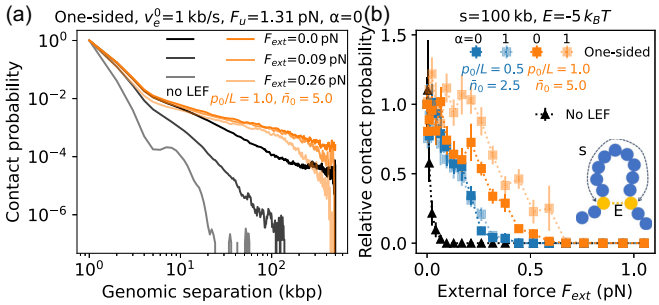


FIG. 2. Polymer structure stabilization by loop extrusion. (a) Contact probability as a function of genomic separation for different loop-extrusion activities and external forces. (b) Relative contact probability between two sticky monomers separated by 100 kb, plotted as a function of external force. The relative contact probability is defined as the contact probability normalized by its value at zero force.

interacting via a short-range attraction of $-5\,k_BT$ [Fig. 2(b) and Fig. S8(b) of the Supplemental Material [20]]. We evaluate how the contact probability between these sites is altered by increasing external force, both in the presence and in the absence of loop extrusion. Without loop extrusion, the contact probability between these monomers drops below 5% of its zero-force value at just 0.1 pN. With active loop extrusion, however, this contact remains largely preserved at the same force level. To quantify this stabilizing effect, we define the rupture force as the external force required to reduce the contact probability to 5% of its zero-force value. The rupture force is approximately ∼0.1 pN without loop extrusion, increases to ∼0.4 pN under "low" extrusion activity, and reaches about ∼0.7 pN in the "high"-activity regime. These results demonstrate that loop extrusion significantly enhances the mechanical resilience of chromatin, helping maintain structural integrity under external forces.

E. Loop extrusion controls chromatin relaxation and recovery under stress

We then examined the dynamic response of the chromatin chain under mechanical load using stress-relaxation simulations. After equilibrating the system, we applied a sudden increase in external tension, maintained the applied force for 1000 s, and then abruptly released it to zero [Fig. 3(a)]. By tracking the chain extension over time, we observed a classical viscoelastic response that is well described by a linear Kelvin-Voigt model [Fig. 3(a), insets]. During the pulling phase, the end-to-end extension follows an exponential approach to its steady-state value:

$$x_{\text{ee}}(t > t_1) = x_{\text{ee}}^0(F_{\text{ext}})\left(1 - \exp\left(-\frac{t - t_1}{\tau_{\text{pull}}}\right)\right) + \text{const},$$

where t_1 is the pulling start time, $x_{\text{ee}}^0(F_{\text{ext}})$ is the steady-state extension under applied force, and τ_{pull} is the characteristic relaxation time during force application. Upon force removal at time t_2, the chain recoils exponentially:

$$x_{\text{ee}}(t > t_2) = x_{\text{ee}}^0(F_{\text{ext}}) \exp\left(-\frac{t - t_2}{\tau_{\text{recoil}}}\right) + \text{const},$$

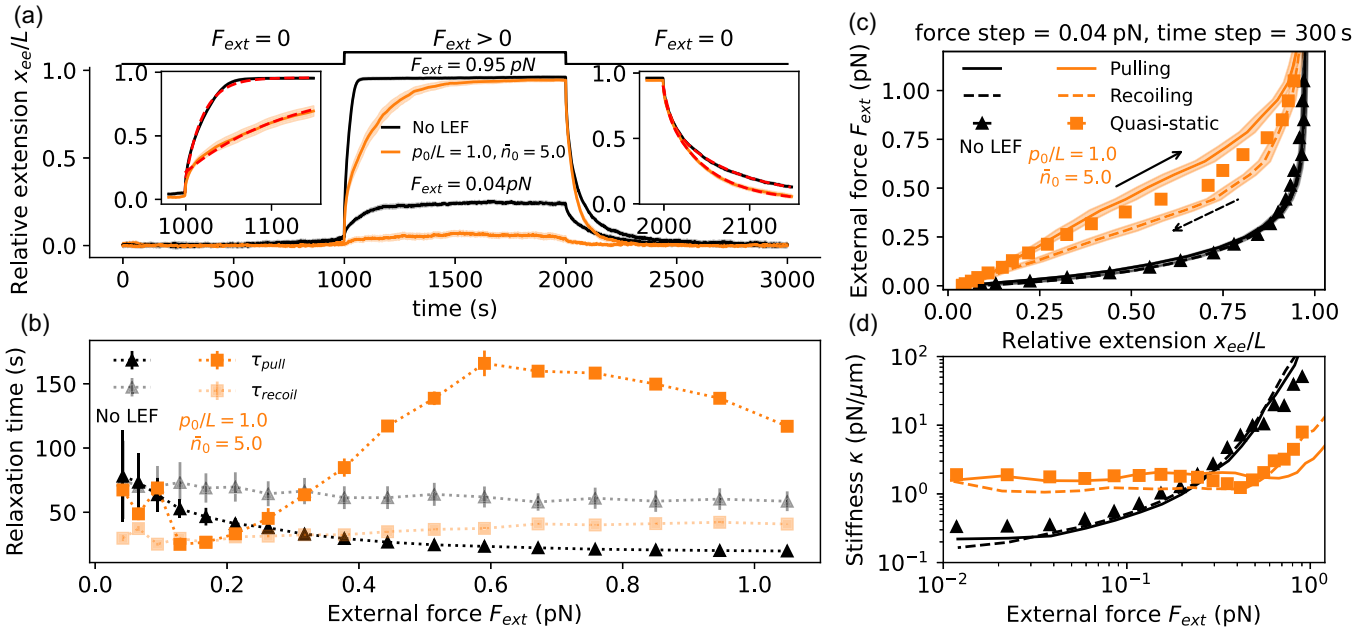


FIG. 3. Dynamic response of a polymer with loop extrusion under external force. (a) Relative extension as a function of time for different levels of loop-extrusion activity. The external force is held at zero from 0 to 1000 s, then suddenly increased at $t_1 = 1000$ s and maintained constant until $t_2 = 2000$ s, after which it is abruptly set back to zero and held from 2000 to 3000 s. Two representative force magnitudes are shown: low force (0.04 pN) and high force (0.95 pN). Insets highlight the extension dynamics during the transition periods in the high-force case, with exponential fits shown as red dashed lines. (b) Characteristic relaxation times during pulling and release phases, obtained from exponential fits, plotted as a function of applied force for varying loop-extrusion activities. (c) Force-extension curves for both pulling and recoiling phases under different loop-extrusion activities, when the applied tension is changed by discrete steps of 0.04 pN every 300 s, highlighting the emergence of hysteresis. (d) Effective stiffness as a function of external force, derived from the curves in panel (c).

where τ_{recoil} denotes the relaxation time in the unloading phase. Both relaxation times are inversely related to the effective stiffness of the chain, i.e., $\tau_{\text{pull}}, \tau_{\text{recoil}} \sim 1/\kappa$.

In the absence of loop extrusion, we find that $\tau_{\text{recoil}} > \tau_{\text{pull}}$, indicating that the chain responds more quickly to the application of force than to its release [Fig. 3(b)]. Moreover, τ_{pull} decreases with increasing external tension, reflecting a force-induced stiffening of the chromatin chain and a nonlinear viscoelastic response. In contrast, τ_{recoil} remains largely independent of the applied force, suggesting that it is governed by the zero-force stiffness of the elastic chain and the intrinsic relaxation dynamics of the entire chain.

When loop extrusion is active, this behavior is reversed: we observe $\tau_{\text{pull}} > \tau_{\text{recoil}}$ [Fig. 3(b)]. Furthermore, τ_{pull} exhibits a nonmonotonic dependence on force: increasing at low to intermediate forces and then decreasing at higher forces. This trend becomes more pronounced with higher loop-extrusion activity [Fig. S9 of the Supplemental Material [20]] and reflects the nonmonotonic force-stiffness relationship observed in extruding chains. Notably, τ_{recoil} is reduced relative to the nonextruding case, reflecting a higher stiffness due to loop-induced compaction in the absence of external load.

At high forces ($\gtrsim$0.2 pN), τ_{pull} in the presence of loop extrusion exceeds that in the absence of loop extruders. This suggests a delayed deformation response due to structural constraints imposed by persistent loops. In contrast, the chain relaxes more rapidly when the force is removed, highlighting the system's ability to efficiently return to compact configurations. These results suggest that loop extrusion protects chromatin integrity under load by resisting deformation and promoting rapid structural recovery, effectively preserving the chromatin conformation under mechanical stress.

F. Hysteresis in extruded chromatin under tension

The out-of-equilibrium, dynamical response of extruded chromatin can also be observed by studying the FE behavior, but in a nonquasistatic way, i.e., without allowing the system to reach a full steady state while increasing or decreasing the applied tension [Fig. 3(c) and Fig. S10 of the Supplemental Material [20]]. A hysteresis cycle is observed, the system keeping the memory of the previous more compact or more elongated state when the external force is gradually augmented or reduced, respectively. Interestingly, the nonmonotonicity of the effective stiffness κ during the pulling and recoiling phases is much less pronounced, and the polymer is stiffer when pulling up to high forces ($\sim$0.7 pN) [Fig. 3(d)].

IV. CONCLUSIONS

We have introduced a force-dependent loop-extrusion model and demonstrated its substantial impact on chromatin mechanics. Our key finding is that loop extrusion significantly alters the stiffness of chromatin in a force-dependent and nonmonotonic manner: Extrusion stiffens the chromatin at low forces but softens it at intermediate and high forces. This behavior is characteristic of the force-extension curve of polymers with internal stored length [27], such as RNA molecules whose internal secondary structures may unzip at high forces [28].

Our analytical model indicates that this effect primarily arises from force-dependent variations in the effective contour length of the chain. The predictions are qualitatively consistent with recent *in vitro* force-extension measurements on human mitotic chromosomes [17,19], which are known to be organized through condensin-mediated loop extrusion [29]. However, due to the inherent structural complexity of mitotic chromosomes, a direct quantitative comparison with our simplified model remains challenging. Nevertheless, our results show that a polymer with dynamically extruded loops can reproduce key experimental features, including increased stiffness at low forces, its reduction at higher forces, and a hysteretic force-extension response consistent with our out-of-equilibrium pulling and recoiling simulations.

We show that loop extrusion not only compacts chromatin structurally but also enhances its mechanical robustness—resisting deformation under sudden stress and promoting rapid structural recovery. This dual role may be critical for maintaining chromosome architecture and safeguarding essential cellular processes, such as transcription and replication, against mechanical perturbations. Our findings suggest experimental directions to explore how chromatin responds to mechanical stress *in vivo* [18], particularly in cells lacking or overexpressing key loop-extruding factors.

ACKNOWLEDGMENTS

We are grateful to Chunlong Chen, John Marko, and members of the Jost group for fruitful discussions. We acknowledge Agence Nationale de la Recherche (Grants No. ANR-21-CE45-0011 and No. ANR-22-CE12-0035) for funding. We thank Centre Blaise Pascal de simulation et modélisation numérique of the ENS de Lyon for computing resources.

DATA AVAILABILITY

The data that support the findings of this article are openly available [30].

[1] J. Zuin, G. Roth, Y. Zhan, J. Cramard, J. Redolfi, E. Piskadlo, P. Mach, M. Kryzhanovska, G. Tihanyi, H. Kohler *et al.*, Nonlinear control of transcription through enhancer–promoter interactions, Nature (London) **604**, 571 (2022).

[2] D. J. Emerson, P. A. Zhao, A. L. Cook, R. J. Barnett, K. N. Klein, D. Saulebekova, C. Ge, L. Zhou, Z. Simandi, M. K. Minsk *et al.*, Cohesin-mediated loop anchors confine the locations of human replication origins, Nature (London) **606**, 812 (2022).

[3] A. Piazza, H. Bordelet, A. Dumont, A. Thierry, J. Savocco, F. Girard, and R. Koszul, Cohesin regulates homology search during recombinational DNA repair, Nat. Cell Biol. **23**, 1176 (2021).

[4] C. Arnould, V. Rocher, F. Saur, A. S. Bader, F. Muzzopappa, S. Collins, E. Lesage, B. Le Bozec, N. Puget, T. Clouaire *et al.*, Chromatin compartmentalization regulates the response to DNA damage, Nature (London) **623**, 183 (2023).

[5] B. Akiyoshi, K. K. Sarangapani, A. F. Powers, C. R. Nelson, S. L. Reichow, H. Arellano-Santoyo, T. Gonen, J. A. Ranish, C. L. Asbury, and S. Biggins, Tension directly stabilizes reconstituted kinetochore-microtubule attachments, Nature (London) **468**, 576 (2010).

[6] Y. Kalukula, A. D. Stephens, J. Lammerding, and S. Gabriele, Mechanics and functional consequences of nuclear deformations, Nat. Rev. Mol. Cell Biol. **23**, 583 (2022).

[7] B. Maier, D. Bensimon, and V. Croquette, Replication by a single DNA polymerase of a stretched single-stranded DNA, Proc. Natl. Acad. Sci. USA **97**, 12002 (2000).

[8] H. Yin, M. D. Wang, K. Svoboda, R. Landick, S. M. Block, and J. Gelles, Transcription against an applied force, Science **270**, 1653 (1995).

[9] D. Saintillan, M. J. Shelley, and A. Zidovska, Extensile motor activity drives coherent motions in a model of interphase chromatin, Proc. Natl. Acad. Sci. USA **115**, 11442 (2018).

[10] C. Dekker, C. H. Haering, J.-M. Peters, and B. D. Rowland, How do molecular motors fold the genome?, Science **382**, 646 (2023).

[11] S. S. Rao, S.-C. Huang, B.G. St Hilaire, J. M. Engreitz, E. M. Perez, K.-R. Kieffer-Kwon, A. L. Sanborn, S. E. Johnstone, G. D. Bascom, I. D. Bochkov *et al.*, Cohesin loss eliminates all loop domains, Cell **171**, 305 (2017).

[12] M. Gabriele, H.B. Brandão, S. Grosse-Holz, A. Jha, G.M. Dailey, C. Cattoglio, T.-H.S. Hsieh, L. Mirny, C. Zechner, and A.S. Hansen, Dynamics of CTCF- and cohesin-mediated chromatin looping revealed by live-cell imaging, Science **376**, 496 (2022).

[13] I. F. Davidson, B. Bauer, D. Goetz, W. Tang, G. Wutz, and J.-M. Peters, DNA loop extrusion by human cohesin, Science **366**, 1338 (2019).

[14] M. Ganji, I. A. Shaltiel, S. Bisht, E. Kim, A. Kalichava, C. H. Haering, and C. Dekker, Real-time imaging of DNA loop extrusion by condensin, Science **360**, 102 (2018).

[15] F. Conforto, Y. Gutierrez Fosado, and D. Michieletto, Fluidification of entangled polymers by loop extrusion, Phys. Rev. Res. **6**, 033160 (2024).

[16] D. Breoni, C. Kurzthaler, B. Liebchen, H. Löwen, and S. Mandal, Giant activity-induced elasticity in entangled polymer solutions, Nat. Commun. **16**, 5305 (2025).

[17] C. F. Nielsen, H. Witt, A. Ridolfi, B. Kempers, E. M. Chameau, S. van der Smagt, M. Barisic, E. J. Peterman, G. J. Wuite, and I. D. Hickson, Condensin I confers stiffness and centromeric cohesion to mitotic chromosomes, bioRxiv. https://www.biorxiv.org/content/10.1101/2025.04.29.651176v1

[18] V.I. Keizer, S. Grosse-Holz, M. Woringer, L. Zambon, K. Aizel, M. Bongaerts, F. Delille, L. Kolar-Znika, V.F. Scolari, S. Hoffmann *et al.*, Live-cell micromanipulation of a genomic locus reveals interphase chromatin mechanics, Science **377**, 489 (2022).

[19] A. E. Meijering, K. Sarlos, C. F. Nielsen, H. Witt, J. Harju, E. Kerklingh, G. H. Haasnoot, A. H. Bizard, I. Heller, C. P. Broedersz *et al.*, Nonlinear mechanics of human mitotic chromosomes, Nature (London) **605**, 545 (2022).

[20] See Supplemental Material at http://link.aps.org/supplemental/10.1103/qfdv-vhv1 for additional method and figures.

[21] H. Salari, M. Di Stefano, and D. Jost, Spatial organization of chromosomes leads to heterogeneous chromatin motion and drives the liquid- or gel-like dynamical behavior of chromatin, Genome Res. **32**, 28 (2022).

[22] H. Salari, G. Fourel, and D. Jost, Transcription regulates the spatio-temporal dynamics of genes through micro-compartmentalization, Nat. Commun. **15**, 5393 (2024).

[23] G. Fudenberg, M. Imakaev, C. Lu, A. Goloborodko, N. Abdennur, and L. Mirny, Formation of chromosomal domains by loop extrusion, Cell Rep. **15**, 2038 (2016).

[24] G. Pobegalov, L.-Y. Chu, J.-M. Peters, and M.I. Molodtsov, Single cohesin molecules generate force by two distinct mechanisms, Nat. Commun. **14**, 3946 (2023).

[25] A. Bonato, J.-W. Jang, D.-G. Kim, K.-W. Moon, D. Michieletto, and J.-K. Ryu, Spontaneously directed loop extrusion in SMC complexes emerges from broken detailed balance and anisotropic DNA search, Nucleic Acids Res. **53**, gkaf725 (2025).

[26] S. B. Smith, L. Finzi, and C. Bustamante, Direct mechanical measurements of the elasticity of single DNA molecules by using magnetic beads, Science **258**, 1122 (1992).

[27] S. Cocco, J. Marko, R. Monasson, A. Sarkar, and J. Yan, Force-extension behavior of folding polymers, Eur. Phys. J. E **10**, 249 (2003).

[28] P. Rissone, C. V. Bizarro, and F. Ritort, Stem–loop formation drives RNA folding in mechanical unzipping experiments, Proc. Natl. Acad. Sci. USA **119**, e2025575119 (2022).

[29] K. Samejima, J. H. Gibcus, S. Abraham, F. Cisneros-Soberanis, I. Samejima, A. J. Beckett, N. Pučeková, M. A. Abad, C. Spanos, B. Medina-Pritchard *et al.*, Rules of engagement for condensins and cohesins guide mitotic chromosome formation, Science **388**, eadq1709 (2025).

[30] https://github.com/physical-biology-of-chromatin/ForceExtensionLoopExtrusion.